Spectrochimica Acta Part A: Molecular and Biomolecular Spectroscopy 135 (2015) 953–958

Contents lists available at ScienceDirect

Spectrochimica Acta Part A: Molecular and Biomolecular Spectroscopy

journal homepage: www.elsevier.com/locate/saa

Investigations into the bovine serum albumin binding and fluorescence properties of Tb (III) complex of a novel 8-hydroxyquinoline ligand

Mingming Zhao [a,b], Ruiren Tang [a,*], Shuai Xu [a]

[a] School of Chemistry and Chemical Engineering, Central South University, Changsha 410083, PR China
[b] Hunan Police Academy, Changsha 410138, PR China

HIGHLIGHTS

- A novel 8-HQ ligand and its Tb (III) complex were synthesized and characterized.
- The fluorescence properties of Tb (III) complex was studied.
- The binding characteristics of $Na_4Tb(\mathbf{L})_2Cl_4{\cdot}3H_2O$ with BSA was investigated.
- Investigating the structural changes of BSA by CD spectra.

GRAPHICAL ABSTRACT

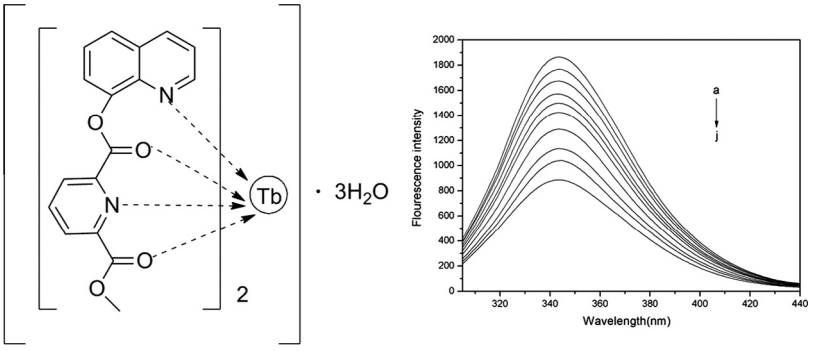

ARTICLE INFO

Article history:
Received 19 April 2014
Received in revised form 12 July 2014
Accepted 29 July 2014
Available online 9 August 2014

Keywords:
8-Hydroxyquinoline
Tb (III) complex
Fluorescence property
BSA binding study
Circular dichroism spectroscopy

ABSTRACT

A novel ligand, 2-methyl-6-(8-quinolinyl)-dicarboxylate pyridine (**L**), and its corresponding Tb (III) complex, $Na_4Tb(\mathbf{L})_2Cl_4{\cdot}3H_2O$, were successfully prepared and characterized. The luminescence spectra showed that the ligand **L** was an efficient sensitizer for Tb (III) luminescence. The interaction of the complex with bovine serum albumin (BSA) was investigated through fluorescence spectroscopy under physiological conditions. The Stern–Volmer analysis indicated that the fluorescence quenching was resulted from static mechanism. The binding sites (n) approximated 1.0 and this meant that interaction of $Na_4Tb(\mathbf{L})_2Cl_4{\cdot}3H_2O$ with BSA had single binding site. The results showed van der Waals interactions and hydrogen bonds played major roles in the binding reaction. Furthermore, circular dichroism (CD) spectra indicated that the conformation of BSA was changed.

Introduction

Since a brightly photoluminescent lanthanide complex was first reported by Weissman in 1942 [1], the properties of lanthanide organic complexes had been extensively studied. Within recently years, lanthanide complexes have enormous applications in many areas, such as chemical, medical, and sensor application [2,3]. The absorption and emission spectra intensity of the trivalent rare earth ions (RE(III)) are weak since intra-configuration 4f–4f transitions in trivalent lanthanide ions are forbidden (Laporte rule). In order to overcome this drawback and obtain outstanding luminescent properties, an organic ligand with excellent absorption coefficient and high efficient ligand-to-RE(III) ions energy transfers, which acts as an "antenna" [4], is very necessary. Based on different ligands and the central RE(III), many novel ligands and complexes have been designed and synthesized [5]. Some of that have excellent lanthanide binding capacity and antenna effects. 8-Hydroxyquinoline (8-HQ) is one of the most important chelates for metal ions and has significant applications in a variety of

* Corresponding author. Tel.: +86 731 88836961; fax: +86 731 88879616.
E-mail address: trr@mail.csu.edu.cn (R. Tang).

http://dx.doi.org/10.1016/j.saa.2014.07.089
1386-1425/

investigations involving metal complexes [6]. It can be matched the first main group of metal ions, transition metal ions, rare earth metal ions [7–9]. 8-HQ has a great conjugate structure so that it can be part of good antenna ligand [10]. It has been used to build lots of highly sensitive fluorescent chemosensors and photoelectric materials [11–13]. On the other hand, 2,6-dipicolinic acid (DPA) is an excellent lanthanide binding substance whose N and O atoms have strong coordination ability in coordination reaction [14,15]. Meanwhile, it possesses biological activity in the body of the animal and plant [16–18]. Its derivatives and complexes are studied extensively and used in all sorts of fields [19]. Taking into account the above advantages of 8-hydroxyquinoline and 2,6-dipicolinic acid, we designed and synthesized a new ligand combining 8-HQ ligand and DPA moieties, expecting it has excellent lanthanide binding capacity and antenna effects.

As one of the most abundant carrier proteins, serum albumin plays an important role in the transport and disposition of endogenous and exogenous ligands present in blood [20,21]. Recently, the interactions of serum albumin with lanthanide complexes have arose much interest owing to their applications in a great deal of medical and chiroptical systems [22]. So, it is very meaningful to explore the action mode between $Na_4Tb(\mathbf{L})_2Cl_4{\cdot}3H_2O$ and bovine serum albumin (BSA), which can provide a theoretical basis for their potential medicinal value.

Here, in order to provide a clue for drug design and pharmaceutical research in this work, the novel ligand of 2-methyl-6-(8-quinolinyl)-dicarboxylate pyridine (**L**) and its Tb (III) complex were designed and synthesized (Scheme 1). The fluorescence property of the complex was researched in detail. Furthermore, the interactions of the complex with BSA were investigated through fluorescence quenching, binding sites, binding mode, CD spectra under physiological conditions, etc.

Experimental

Materials

8-Hydroxyquinoline (8-HQ) was purchased from Beijing (China) Medicine Co. Ltd.; BSA, obtained from Sigma Chemical Co. Ltd., was dissolved in 0.1 M Tris–HCl buffer solution (pH = 7.40, 50 mM NaCl). BSA stock solution (1.0×10^{-5} mol/L) was kept in the fridge at 0–4 °C. And other chemicals were of A.R. grade without further purification. Doubly distilled and deionized water were used in the whole experiments.

Melting points were determined on a XR-4 apparatus (thermometer uncorrected); Elemental analysis was carried out by a Perkin Elmer 2400 elemental analyzer; Infrared spectra were recorded on a Nicolet NEXUS 670 FT-IR spectrophotometer using KBr discs in the 400–4000 cm^{-1} region; ^1H NMR and ^{13}C NMR spectra were measured with a Bruker-400 MHz nuclear magnetic resonance spectrometer with $CDCl_3$ as solvent and TMS as internal reference.

Luminescence measurements were made on a Hitich F-4500 spectrophotometer, the widths of both the excitation and emission slit were set to 5 nm with the photomultiplier tube voltage at 700 V. Thermal gravimetric analysis (TGA) were performed in the nitrogen atmosphere using a Netzsch TG 209 thermal gravimetric analyzer at a heating rate of 10 °C min^{-1} from 25 to 750 °C. CD measurements were carried out on a J-810 spectropolarimeter (Jasco, Tokyo, Japan) in a cell of path length 1.0 mm at room temperature.

Preparation of ligand (L)

Synthesis of 6-(methoxycarbonyl)-pyridine-2-carboxylic acid (2)

A solution of (1) (5.85 g, 30.0 mmol) in methanol (150 mL) was cooled to 0 °C. After KOH pellets (1.76 g, 31.0 mmol) were added, the reaction mixture was stirred at 0 °C for 2 h and then at room temperature for 24 h. The solvent was removed under reduced pressure, and the residue was suspended in H_2O (100 mL) and extracted with ethyl acetate (3 × 30 mL). The aqueous layers were acidified to pH 3 with 1 M diluted HCl solution and extracted with chloroform (5 × 30 mL). The collected organic layers were dried over anhydrous Na_2SO_4. The chloroform was removed in vacuum to provide the desired product as a white solid (2.80 g, yield: 52%). m.p. 144–146 °C; ^1H NMR (400 MHz, $CDCl_3$): δ 8.45 (m, 2*H*, Py-3, 5), 8.18 (t, *J* = 6.50 Hz, 1*H*, Py-4), 3.93 ppm (s, 3*H*, CH_3); IR (KBr), v/cm^{-1}: 3073, 2964, 2852, 1725, 1581, 1325.

Synthesis of 2-methyl-6-(8-quinolinyl)-dicarboxylate pyridine (L)

8-Hydroxyquinoline (8-HQ) (1.6 g, 11 mmol) and (2) (2.0 g, 11 mmol) were dissolved in 60 mL of CH_2Cl_2 (CH_2Cl_2, dried by P_2O_5) at room temperature. To this stirring solution was slowly added DMAP (0.27 g, 3 mmol) and 20 mL of a solution of 2.53 g (13 mmol) of EDC·HCl in CH_2Cl_2 under dried condition at room temperature. After 48 h of stirring, organic phase was washed by water (3 × 30 ml) to clear out EDC·HCl and DMAP. A white precipitate was obtained by evaporated under pressure. The grey solid was recrystallized over AcOEt and petroleum ether. The white product was recrystallized over acetone and H_2O to give the title compound (**L**) (1.90 g, yield:56%). m.p. 157–159 °C; ^1H NMR (400 MHz, $CDCl_3$): δ 8.88(d, *J* = 3.60 Hz, 1*H*, 8-HQ-2), 8.62 (m, 2*H*, Py-3, 5), 8.25 (t, *J* = 6.50 Hz, 1*H*, Py-4), 8.11–7.46 (m, 5*H*, 8-HQ-3,4,5,2,7), 4.06 ppm (s, 3*H*, CH_3); ^{13}C NMR(400 MHz, $CDCl_3$): δ 52.9 (CH_3); 113.4, 118.9, 123.1, 127.7, 128.8, 128.9, 131.1, 137.3, 138.8, 141.2, 149.0, 149.0, 151.7, 154.2 (all Ph-*C* and Py-*C*), 158.7 (*C*OO-8-HQ), 167.0 ppm (*C*OOCH$_3$); IR (KBr), v/cm^{-1}: 3064, 2955, 1737, 1575, 1232, 1113.

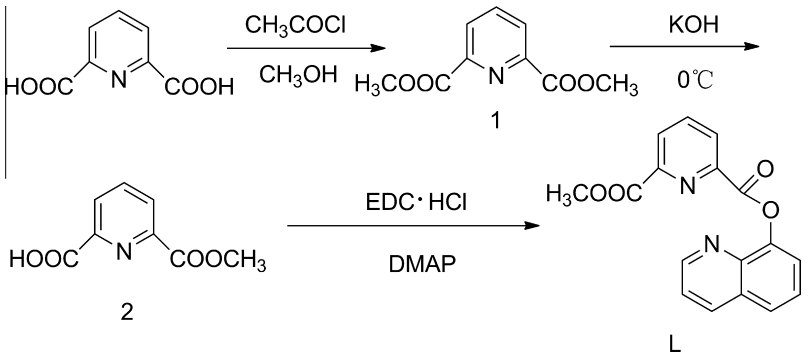

Scheme 1. The synthetic route of ligand **L**.

Synthesis of Tb (III) complex

The complex $Na_4Tb(\mathbf{L})_2Cl_4{\cdot}3H_2O$ was prepared in the following steps. A solution of **L** (1 mmol) in ethanol (10 ml) was added dropwise to the solution of $TbCl_3$ (0.5 mmol) in ethanol (10 ml) under stirring at 60 °C for 24 h. Then the pH value of the mixture was adjusted to 6 by adding an aqueous solution of sodium hydroxide (1 mol/L). The yellow precipitate was collected by filtration, washed three times with ethanol and chloroform mixture (1:1, v:v), dried in vacuum at 60 °C one day.

Results and discussion

Composition and properties of the complex

Elemental analytical

The elemental analytical data for the complex is presented in Table 1, which is in good agreement with the values calculated from the molecular formula, $Na_4Tb(\mathbf{L})_2Cl_4{\cdot}3H_2O$. The complex is yellowish powder, stable under atmospheric condition and soluble in DMF, DMSO and methanol, a little soluble in H_2O and acetone, insoluble in benzene, diethyl ether and toluene.

FT-IR spectra

The FT-IR spectra and characteristic absorption bands of the free ligand **L** and its Tb (III) complex are shown in Fig. 1 and Table 2. The FT-IR spectra of the free ligand **L** shows bands 1738 cm^{-1}, 1579 cm^{-1}, 1500 cm^{-1}, 1231 cm^{-1}, which can be assigned to ν(C═O), ν_{Py}(C═N), $\nu_{8\text{-HQ}}$(C═N) and ν(C—N) of the ligand, respectively. Two ν(C═O) absorption bands in the ligand **L** are coincided so that only one ν(C═O) absorption bands in the FT-IR spectra. In comparison with the ligand, the FT-IR spectra of the Tb (III) complex are changed greatly, the band ν(C═O) at 1738 cm^{-1} in free ligand disappears and the new band appears at 1625 cm^{-1}. The absorption band assign to the coordinated ν(Tb—O) is found at around 489 cm^{-1}. These evidences clearly show that two carbonyl groups participate in coordination reaction. The bands ν_{Py} (C═N), $\nu_{8\text{-HQ}}$(C═N) and ν(C—N) peak are slightly shifted to 1568 cm^{-1}, 1486 cm^{-1}, 1322 cm^{-1} for the complex $Na_4Tb(\mathbf{L})_2Cl_4{\cdot}3H_2O$. These indicate that pyridine and 8-hydroxyquinoline nitrogen atoms participate in coordination reaction. The band ν(O—H) vibration at 3414 cm^{-1}, is relatively intense and can be assigned to solvated water.

Thermal gravimetric analysis

The thermal gravimetric analysis of the complex is given in Fig. S1. (Fig. S1–S4 are shown in support information). There are two main successive mass loss stages in the TGA curves. The first stage of the decomposition appears within 30–170 °C corresponding to the loss of the solvated water (Weight loss: 5.25%, Calcd: 4.92%). And the second loss stage ranging from 250 to 450 °C is attributed to the loss of *L* (Weight loss: 57.68%, Calcd: 56.20%), which is confirmed by comparing the observed and the calculated mass of the complex. The detailed data are listed in Table 3. Furthermore, the TGA proves that it has the relatively high thermal stability.

The results of EA, TGA and FT-IR spectroscopy indicate that the ligand **L** have two carbonyl groups and two nitrogen atom what involved with the coordination, and the chemical structure of complex may be as shown in Scheme 2.

Table 1
Result of elemental analysis data for Tb (III) complex.

Complex	C, H, N Found (calc.)		
	C (%)	H (%)	N (%)
$Na_4Tb(\mathbf{L})_2Cl_4{\cdot}3H_2O$	37.36 (37.22)	2.80 (2.73)	5.07 (5.11)

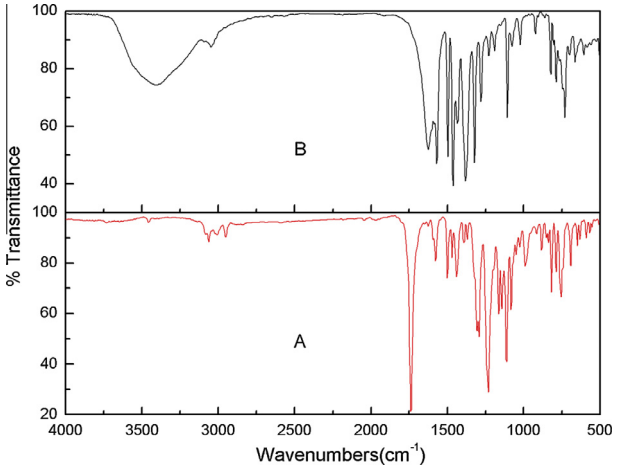

Fig. 1. IR Spectrum of ligand **L** and Tb (III) complex. A: L, B: $Na_4Tb(\mathbf{L})_2Cl_4{\cdot}3H_2O$.

Fluorescence properties of complex

The excitation and emission spectra of the Tb (III) complex is examined in C_2H_5OH solution ($c = 2.0 \times 10^{-4}$ mol/L) at ambient temperature (Fig. 2). The luminescence data for the Tb (III) complex are listed in Table 4. The maximum excitation wavelength of the complex $Na_4Tb(\mathbf{L})_2Cl_4{\cdot}3H_2O$ is 277 nm, due to the π–π^* transition centered at the ligand **L**. The complex displays the characteristic line emission of 4f–4f transition of Tb (III) ion, consisting of four main lines at 490 nm ($^5D_4 \rightarrow {}^7F_6$), 545 nm ($^5D_4 \rightarrow {}^7F_5$), 585 nm ($^5D_4 \rightarrow {}^7F_4$) and 621 nm ($^5D_4 \rightarrow {}^7F_3$), and the emission band at 545 nm is obviously stronger than the other emission bands [23]. Still, each emission band is very narrow and the width of half band is about several nanometers, indicating that the complex has high color purity and the ligand is a comparative good organic chelator to sensitize fluorescence of Tb (III) ion [24].

Interactions with BSA

Fluorescence spectrum

A 2.5 mL solution containing 1.0×10^{-5} mol/L BSA was titrated by successive addition of 1.0×10^{-3} mol/L stock solution of $Na_4Tb(\mathbf{L})_2Cl_4{\cdot}3H_2O$ and the concentration of it varied from 0 to 1.4×10^{-4} mol/L. Titrations were done manually by using microinjector. An excitation wavelength (Ex) of 280 nm was chosen in the experiment. The excitation and emission slit widths (5 nm each) and scan rate (240 nm/min) were constantly maintained for all experiments. The fluorescence spectra were recorded at 298 K, 308 K and 318 K in the range of 300–440 nm, respectively. The temperatures of the samples were kept by recycled water throughout the experiment.

Analysis of fluorescence quenching of BSA by the complex

The effect of $Na_4Tb(\mathbf{L})_2Cl_4{\cdot}3H_2O$ on the fluorescence emission spectra of BSA (PH = 7.40) at 298 K is shown in Fig. 3, and the corresponding calculated results are given in Table 5. As shown in Fig. 3, the natural fluorescence of BSA at around 340 nm is gradually quenched by the increasing concentration of the complex, while the complex $Na_4Tb(\mathbf{L})_2Cl_4{\cdot}3H_2O$ has no intrinsic fluorescence in this range. Results above indicate that strong interaction exist between $Na_4Tb(\mathbf{L})_2Cl_4{\cdot}3H_2O$ and BSA, and the microenvironment around the chromophore of BSA is also changed [25]. In order to shed light on the fluorescence quenching mechanism, the

Table 2
Comparison between IR spectra of ligand **L** and complex.

Complex	ν(OH)	ν(C=O)	ν_{Py}(C=N)	$\nu_{8\text{-}HQ}$(C=N)	ν(C—N)	ν(Re—O)
L		1738	1579	1500	1231	
$Na_4Tb(L)_2Cl_4{\cdot}3H_2O$	3414	1625	1568	1486	1322	489

Table 3
TGA data of $Na_4Tb(\mathbf{L})_2Cl_4{\cdot}3H_2O$.

Complex	Stage	Temperature range (°C)	Mass loss (%) found (calc.)	Probable lost molecules
$Na_4Tb(\mathbf{L})_2Cl_4{\cdot}3H_2O$	I	30–170	5.25 (4.92)	$3H_2O$
	II	250–450	57.68 (56.20)	**2L**

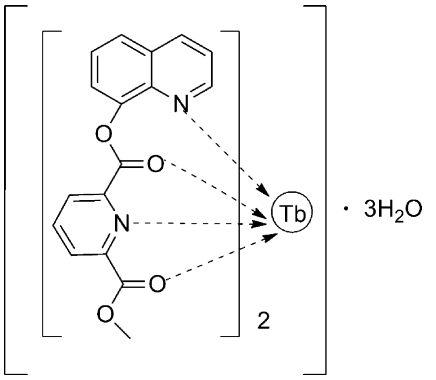

Scheme 2. The chemical structure of $Na_4Tb(\mathbf{L})_2Cl_4{\cdot}3H_2O$.

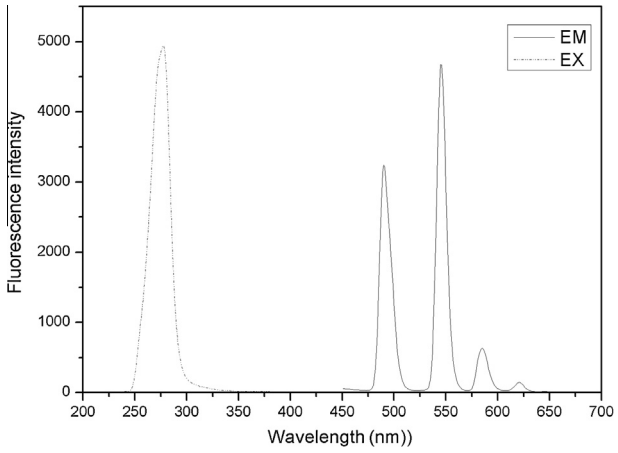

Fig. 2. Excitation (left) and emission (right) spectra of $Na_4Tb(\mathbf{L})_2Cl_4{\cdot}3H_2O$ ($c = 2.0 \times 10^{-4}$ mol/L, C_2H_5OH).

Table 4
Fluorescence data for Tb (III) complex.

Complex	λ_{ex} (nm)	λ_{em} (nm)	F	Assignment
$Na_4Tb(\mathbf{L})_2Cl_4{\cdot}3H_2O$	277	490	3242	$^5D_4$–$^7F_6$
		545	4670	$^5D_4$–$^7F_5$
		585	634	$^5D_4$–$^7F_4$
		621	147	$^5D_4$–$^7F_3$

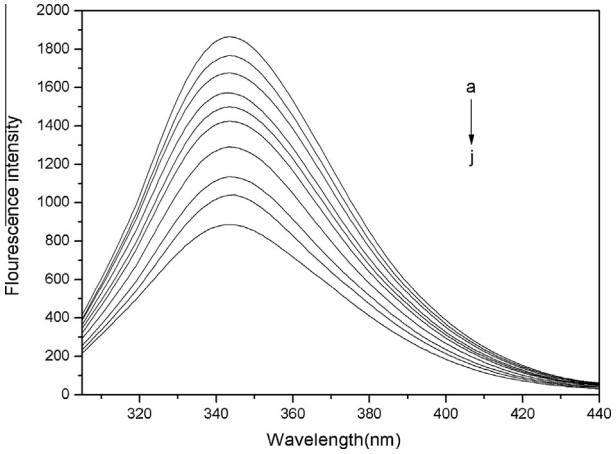

Fig. 3. The quenching effect of $Na_4Tb(\mathbf{L})_2Cl_4{\cdot}3H_2O$ on fluorescence intensity of BSA at 298 K; λ_{ex} = 280 nm; c(BSA) = 1.0×10^{-5} mol/L; c(**L**)/(10^{-5} mol/L). (a–j): 0, 1, 2, 3, 4, 6, 8, 10, 12 and 14, respectively.

Table 5
Fluorescence quenching constants of complex-BSA at three different temperatures.

Complex	T (K)	K_{sv} ($\times 10^4$ L mol^{-1})	k_q ($\times 10^{12}$ L mol^{-1} S^{-1})	[a]R^2
$Na_4Tb(\mathbf{L})_2Cl_4{\cdot}3H_2O$	298	1.05	1.05	0.99607
	308	0.88	0.88	0.99806
	318	0.72	0.72	0.99646

[a] R is the correlation coefficient of Stern–Volmer equation.

fluorescence quenching data are analyzed by the Stern–Volmer equation (Eq. (1)) [26]. The graphs plotted for F_0/F against [Q] from Eq. (1) at different temperatures are shown in Fig. S2.

$$\frac{F_0}{F} = 1 + K_{sv}[Q] = 1 + \tau_0 k_q[Q] \quad (1)$$

where F_0 and F are the fluorescence intensities in the absence and presence of quencher, respectively, K_{sv} is the Sterne–Volmer quenching constant, [Q] is the concentration of quencher, τ_0 is the average fluorescence lifetime of biomolecule at about 10^{-8} s [27]. k_q is the biomolecule quenching rate constant and the value of the maximum scattering collision quenching constant is 2.0×10^{10} L mol^{-1} S^{-1} [28]. The results show the value of k_q is the rate constants of BSA quench by $Na_4Tb(\mathbf{L})_2Cl_4{\cdot}3H_2O$, which is greater than 2.0×10^{10} L mol^{-1} S^{-1}. The slope of the Sterne–Volmer quenching constants (K_{sv}) are 1.05×10^4, 8.8×10^3, 7.2×10^3 (L mol^{-1}) at 298 K, 308 K and 318 K, which inversely correlated with the temperature. These evidences indicate that the main quenching mechanism of BSA by the $Na_4Tb(\mathbf{L})_2Cl_4{\cdot}3H_2O$ should be a static quenching procedure [29].

Binding constant and binding sites

The relationship between fluorescence intensity and the concentration of quenchers can be described by the following Eq. (2) for static quenching, the apparent K_a is the binding constant and n is the number of binding sites per BSA can be expressed [30]:

$$\log\frac{F_0 - F}{F} = \log K_a + n\log[Q] \quad (2)$$

Fig. S3 shows the double-logarithm algorithm curve, the results of K_a and n are listed in Table 6. It is noticed that the binding constant values are equal to 10^4 and decrease with the increase of temperature due to reduction of the stability of $Na_4Tb(\mathbf{L})_2Cl_4{\cdot}3H_2O$-BSA system. On the other hand, the correlation coefficient R is about 0.995,

Table 6
The binding constant (K_a), binding sites (n) and relative thermodynamic parameters for the Tb (III) complex with BSA at three different temperatures.

Complex	T (K)	K_a (L mol^{-1})	n	[b]R^2	ΔH (kJ mol^{-1})	ΔS (J mol^{-1} K^{-1})	ΔG (kJ mol^{-1})	[c]R^2
$Na_4Tb(\mathbf{L})_2Cl_4{\cdot}3H_2O$	298	3.5×10^4	1.18	0.99861			−20.65	
	308	2.5×10^4	1.12	0.99945	−23.26	−8.76	−20.56	0.99521
	318	1.9×10^4	1.08	0.99088			−20.47	

[b] R^2 is the correlation coefficient of double-logarithm equation.
[c] R^2 is the correlation coefficient of the value of ΔH, ΔS.

which proves that the interaction between the complex and BSA is in accordance with the site-binding model underlined in the above equation. The above results clearly indicates that $Na_4Tb(\mathbf{L})_2Cl_4{\cdot}3H_2O$ quenches the fluorescence emission of BSA with higher binding affinity and experiences a static quenching process. The binding capacity (n) varies in the range from 1.08 to 1.18, therefore that the number of binding sites approximates 1.0 and the interaction of $Na_4Tb(\mathbf{L})_2Cl_4{\cdot}3H_2O$ with BSA has single binding site.

Thermodynamic parameters and binding mode

In general, the working forces between the proteins and ligands mainly include four types: hydrophobic force, electrostatic interactions, van der Waals interactions and hydrogen bonds. To illustrate the interaction of **L** with BSA, the thermodynamic parameters (ΔH, ΔS) are calculated from the Van't Hoff equation at three different temperatures [30].

$$\ln K_a = -\frac{\Delta H}{RT} + \frac{\Delta S}{R} \quad (3)$$

where K_a is the effective binding constant at the corresponding temperature and R is the gas constant. The calculation is carried out at three different temperatures, which are 298 K, 308 K, and 318 K. The enthalpy change (ΔH) is calculated from the slope of the *van't Hoff* relationship. The free energy change (ΔG) is then estimated from the following relationship:

$$\Delta G = \Delta H - T\Delta S \quad (4)$$

Fig. S4, by plotting the data in Table 6, shows the values of ΔH and ΔS obtained for the binding site from the slopes and ordinates at the origin of the fitted lines. When $\Delta H < 0$ or $\Delta H \approx 0$, $\Delta S > 0$, the main acting force is electrostatic force; when $\Delta H < 0$, $\Delta S < 0$, the main acting force is van der Waals interactions and hydrogen bonds; when $\Delta H > 0$, $\Delta S > 0$, the main force is hydrophobic force [31]. The negative enthalpy (ΔH) and entropy (ΔS) values of the interaction between $Na_4Tb(\mathbf{L})_2Cl_4{\cdot}3H_2O$ and BSA indicate that van der Waals interactions and hydrogen bonds play major roles in the binding reaction. Furthermore, the negative free energy change ΔG and ΔH suggests the binding process is exothermic and spontaneous.

Circular dichroism spectroscopy

As CD spectra is one of the sensitive methods for monitoring the conformational changes in the protein [32]. The induced ellipticity is obtained by the ellipticity of the $Na_4Tb(\mathbf{L})_2Cl_4{\cdot}3H_2O$–BSA mixture subtracting the ellipticity of $Na_4Tb(\mathbf{L})_2Cl_4{\cdot}3H_2O$ at the same wavelength and expressed in degrees. To quantify the results, the mean residue ellipticity (MRE) in deg cm^2/dmol^{-1}, and the α-helix contents of free and bound BSA are calculated using the following respective equations [33]:

$$\mathrm{MRE} = \theta / C_p n l 10 \quad (5)$$

where θ is the observed dichroism in millidegree, C_p is the molar concentration of the BSA, n is the number of amino acid residues in protein (583) and l is the optical length of the cell (0.1 cm).The α-helical content of BSA is calculated from the MRE value at 208 nm using the equation:

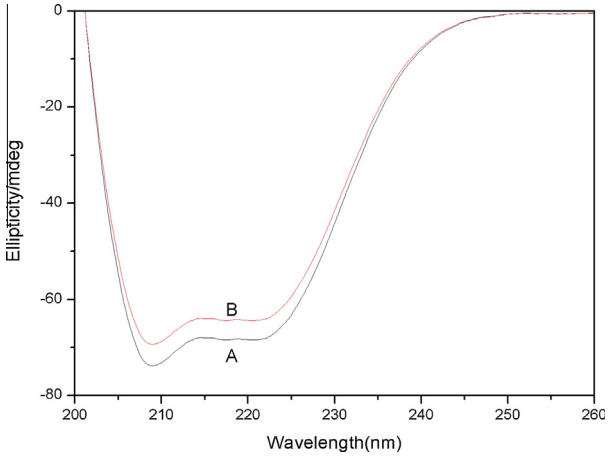

Fig. 4. CD spectra of the BSA–$Na_4Tb(\mathbf{L})_2Cl_4{\cdot}3H_2O$ system at pH 7.40, 298 K. (A) 5.0×10^{-6} mol/L BSA; (B) 5.0×10^{-6} mol/L BSA and 5.0×10^{-6} mol/L $Na_4Tb(\mathbf{L})_2Cl_4{\cdot}3H_2O$.

$$\alpha\%\mathrm{helix} = [(-\mathrm{MRE}_{208} - 4000)/33000 - 4000] \times 100 \quad (6)$$

where MRE_{208} is the MRE value observed at 208 nm, 4000 is the MRE of the β-form and random coil conformation cross at 208 nm, and 33,000 is the MRE value of a pure α-helix at 208 nm [34].

Fig. 4 shows the CD spectra of BSA and BSA–Tb (III) complex, which characteristic features of the typical (α + β) helix structure with negative bands at 208 and 223 nm. The binding of $Na_4Tb(\mathbf{L})_2Cl_4{\cdot}3H_2O$ to BSA cause a decrease in band intensity without any significant shift of the peaks, indicating a decrease of the α-helical content in protein [32]. Using the Eq. (5) and (6), the calculated results exhibit a reduction of α-helix structures from 60.53% to 57.17% at $Na_4Tb(\mathbf{L})_2Cl_4{\cdot}3H_2O$ /BSA molar ratio of 1:1. From the above results, it is apparent that the effect of $Na_4Tb(\mathbf{L})_2Cl_4{\cdot}3H_2O$ on BSA causes a conformational change of the protein, with the loss of α-helical stability.

Conclusions

In summary, a novel ligand, 2-methyl-6-(8-quinolinyl)-dicarboxylate pyridine (**L**), and its corresponding Tb (III) complex were synthesized and characterized by EA, ^{1}H NMR, ^{13}C NMR, FT-IR and TGA. The study of their luminescence properties showed the Tb (III) complex could be sensitized efficiently by the ligand. The interactions of $Na_4Tb(\mathbf{L})_2Cl_4{\cdot}3H_2O$ with BSA were investigated through the fluorescence spectroscopy under physiological conditions. The probable quenching mechanism of the fluorescence of BSA with Tb (III) complex was static quenching and the single binding site. Van der Waals interactions and hydrogen bonds played major roles in the binding reaction. The CD spectra indicated that the interaction of $Na_4Tb(\mathbf{L})_2Cl_4{\cdot}3H_2O$ with BSA caused conformational change of BSA. These results give important insight into interactions of the rare earth complexes and BSA, which shows great reference value for research and application in drug design and pharmacodynamic fields.

Acknowledgement

Financial support from the National Natural Science Foundation of China (No. 21071152, China) is gratefully acknowledged.

Appendix A. Supplementary material

Supplementary data associated with this article can be found, in the online version, at http://dx.doi.org/10.1016/j.saa.2014.07.089.

References

[1] S.I. Weissman, J. Chem. Phys. 10 (1942) 214–217.
[2] V. Tsaryuk, V. Zolin, K. Zhuravlev, V. Kudryashova, J. Legendziewicz, R. Szostak, J. Alloys Compd. 451 (2008) 153–157.
[3] R.X. Ma, Z.M. Chen, Z.H. Gao, R.F. Wang, J.J. Zhang, Synth. Met. 159 (2009) 1272–1276.
[4] E. Niyama, H.F. Brito, M. Cremona, Spectrochim. Acta A 61 (2005) 2643–2649.
[5] C.M.G. dos Santos, A.J. Harte, S.J. Quinn, T. Gunnlaugsson, Coordin. Chem. Rev. 252 (2008) 2512–2527.
[6] M. Iwamuro, Y. Wada, T. Kitamura, T.J. Adachi, Chem. Lett. 28 (1999) 539–540.
[7] C. Schmitz, H.W. Schmidt, M.J. Thelakkat, Chem. Mater. 12 (2000) 3012–3019.
[8] E. Garribba, G. Micera, D. Sanna, E. Lodyga-Chruscinska, Inorg. Chim. Acta 348 (2003) 97–106.
[9] R.I.R. Blyth, J. Thompson, Y. Zou, R. Fink, E. Umbach, G. Gigli, R. Cingolani, Synth. Met. 139 (2003) 207–213.
[10] H.B. Xu, J. Li, L.X. Shi, Z.N. Chen, Dalton Trans. 40 (2011) 5549–5556.
[11] M.D. Shults, B. Imperiali, J. Am. Chem. Soc. 125 (2003) 14248–14249.
[12] S.Y. Moon, N.R. Cha, Y.H. Kim, S.K. Chang, J. Org. Chem. 69 (2004) 181–183.
[13] H. Zhang, L.F. Han, K.A. Zachariasse, Y.B. Jiang, Org. Lett. 19 (2005) 4217–4220.
[14] L.Q. Shen, Z.F. Yang, R.R. Tang, Spectrochim. Acta A 98 (2012) 170–177.
[15] Y.M. Luo, J. Li, L.X. Xiao, R.R. Tang, X.C. Tang, Spectrochim. Acta A 72 (2009) 703–708.
[16] X.C. Su, H.B. Liang, S. Simonsen, J. Am. Chem. Soc. 130 (2008) 10486–10487.
[17] U. Karhunen, J. Rosenberg, U. Lamminmaki, T. Soukka, Anal. Chem. 83 (2011) 9011–9016.
[18] Q.F. Li, Y. Yang, A. Maleckis, G. Otting, X.C. Su, Chem. Commun. 48 (2012) 2704–2706.
[19] S.S. Krishnmurthy, S. Soundarajan, Z. Anorg, Allg. Chem. 348 (1996) 309–312.
[20] D.C. Carter, J.X. Ho, Adv. Protein Chem. 45 (1994) 153–203.
[21] L.A. MacManus-Spencer, M.L. Tse, P.C. Hebert, H.N. Bischel, R.G. Luthy, Anal. Chem. 82 (2010) 974–981.
[22] G. Zolese, G. Falcioni, E. Bertoli, R. Wozniak, Z. Wypych, E. Gratton, A. Ambrosini, Proteins 40 (2000) 39–48.
[23] T.Y. Zhu, K. Ikarashi, T. Ishigaki, K. Uematsu, K. Toda, H. Okawa, M. Sato, Inorg. Chim. Acta 362 (2009) 3407–3414.
[24] Z.F. Zhang, R.R. Tang, J. Mol. Struct. 1010 (2012) 116–122.
[25] T.H. Wang, Z.M. Zhao, L. Zhang, L. Ji, J. Mol. Struct. 937 (2009) 65–69.
[26] Y.C. Liu, Z.Y. Yang, J. Organomet. Chem. 694 (2009) 3091–3101.
[27] N. Zhou, Y.Z. Liang, P. Wang, J. Photochem. Photobiol. A 185 (2007) 271–276.
[28] W.R. Ware, J. Phys. Chem. 66 (1962) 455–458.
[29] X.J. Guo, X.W. Han, J. Tong, C. Guo, W.F. Yang, J.F. Zhu, B. Fu, J. Mol. Struct. 966 (2010) 129–135.
[30] Y.J. Hu, O.Y. Yu, A.M. Bai, R.M. Zhao, Y. Liu, Biol. Trace Elem. Res. 136 (2010) 8–10.
[31] Y.T. Sun, H.T. Zhang, Y. Sun, Y.P. Zhang, H. Liu, J.H. Cheng, S.Y. Bi, H.Q. Zhang, J. Lumin. 130 (2010) 270–279.
[32] H. Gao, L.D. Lei, J.Q. Liu, Q. Kong, X.G. Chen, Z.D. Hu, J. Photochem. Photobiol. A 167 (2004) 213–221.
[33] Y. Li, W. He, J. Liu, F. Sheng, Z. Hu, X. Chen, Biochim. Biophys. Acta 1722 (2005) 15–21.
[34] Z.X. Lu, T. Cui, Q.L. Shi, First ed., Science Press, Beijing, 1987.